

ViT-AdaLA: Adapting Vision Transformers with Linear Attention

Yifan Li^{1,2} Seunghyun Yoon² Viet Dac Lai² Franck Deroncourt² Jason Kuen² Yu Kong¹ Trung Bui²

Abstract

Vision Transformers (ViTs) based vision foundation models (VFMs) have achieved remarkable performance across diverse vision tasks, but suffer from quadratic complexity that limits scalability to long sequences. Existing linear attention approaches for ViTs are typically trained from scratch, requiring substantial computational resources, while linearization-based methods developed for large language model decoders do not transfer well to ViTs. To address these challenges, we propose **ViT-AdaLA**, a novel framework for effectively adapting and transferring prior knowledge from VFMs to linear attention ViTs. ViT-AdaLA consists of three stages: attention alignment, feature alignment, and supervised fine-tuning. In the attention alignment stage, we align vanilla linear attention with the original softmax-based attention in each block to approximate the behavior of softmax attention. However, residual approximation errors inevitably accumulate across layers. We mitigate this by fine-tuning the linearized ViT to align its final-layer features with a frozen softmax VFM teacher. Finally, the adapted prior knowledge is transferred to downstream tasks through supervised fine-tuning. Extensive experiments on classification and segmentation tasks demonstrate the effectiveness and generality of ViT-AdaLA over various state-of-the-art linear attention counterpart.

1. Introduction

Vision Transformers (ViTs) (Dosovitskiy et al., 2020) based vision foundation models (VFMs) such as DINOv2 (Oquab et al., 2024) and CLIP (Radford et al., 2021) have been widely adopted across a broad range of computer vision tasks (Li et al., 2025c), including segmentation, detection, visual question answering (VQA), depth estimation, and image, video, and 3D point-cloud generation. However, the

¹Michigan State University, East Lansing, MI, USA. ²Adobe Research. Correspondence to: Yifan Li <liyifa11@msu.edu>.

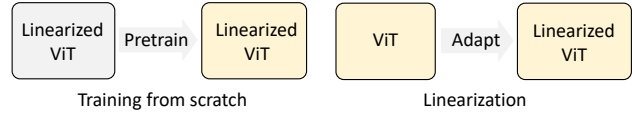


Figure 1. Comparison between training-from-scratch and linearization paradigms for ViTs with linear attention. Training-from-scratch linear attention paradigms focus on designing accurate attention approximation methods, which typically require large-scale pretraining to acquire strong prior knowledge. In contrast, ViT linearization leverages an off-the-shelf pretrained ViT, substantially reducing the need for extensive pretraining.

standard softmax-based self-attention in ViTs scales quadratically with the number of visual tokens, leading to substantial computational and memory overhead as the sequence length increases as shown in Fig. 3. This limitation becomes increasingly acute as modern vision applications demand processing long-sequence visual tokens.

To address the computational and memory bottlenecks of ViTs, extensive efforts have been devoted to improving the efficiency of softmax-based self-attention, including attention matrix optimization (Dao et al., 2022b), token reduction methods (Rao et al., 2021), distillation (Touvron et al., 2021), sliding-window mechanisms (Liu et al., 2021), sequence modeling approaches (Gu & Dao, 2023), and linear attention variants (Katharopoulos et al., 2020). Among these, linear attention methods are particularly attractive, as they reduce the quadratic complexity ($\mathcal{O}(N^2D)$), to linear complexity ($\mathcal{O}(ND^2)$), where N and D indicate the sequence length and the feature dimension, respectively. Existing linear attention approaches can be categorized into two types (Fig. 1): training from scratch (Yaras et al., 2025; Xiong et al., 2021) and linearization (Zhang et al., 2024; 2025; Liu et al., 2025; Lan et al., 2025; Goldstein et al., 2025). The former focuses on designing accurate softmax-approximation methods, and trains a linearized ViT entirely from scratch, typically requiring large-scale pretraining before fine-tuning on downstream tasks, especially for the VFMs designed as general-purpose feature extractors. Without such extensive pretraining, these approaches often suffer from severe performance degradation when directly adapted to downstream scenarios (see Tab. 1, 2, 4), limiting their practicality under realistic data and compute constraints. The latter, in contrast, inherits prior knowledge from the softmax-based VFMs and therefore requires substantially

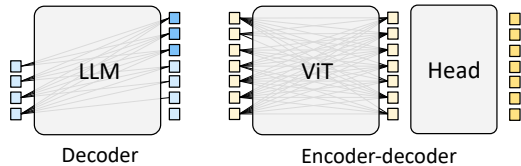


Figure 2. Comparison of decoder and encoder-decoder architectures. In decoder-based LLMs, the LLM serves as both the feature extractor and the target generator. In contrast, in vision models, ViTs function solely as feature extractors, while a separate task-specific head is responsible for target generation.

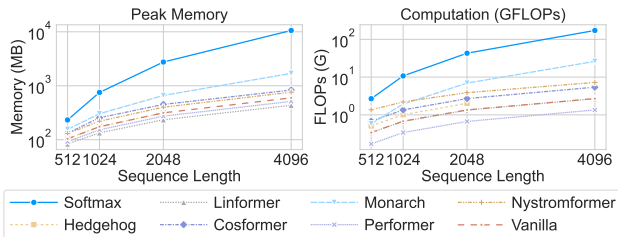


Figure 3. Efficiency comparison of different attentions, including peak memory and GFLOPs varying with sequence length. Only attention module is benchmarked in these experiments. “Vanilla” indicates the vanilla linear attention (Katharopoulos et al., 2020).

fewer pretraining steps than training-from-scratch methods.

However, existing work on linearization stream such as LoL-CATS (Zhang et al., 2025) has primarily focused on large language models (LLMs), which are decoder-based transformers and differ fundamentally from encoder-decoder-based vision models (see Fig. 2). In decoder-only LLMs, the model acts as both a feature extractor and a target generator, whereas in vision models, the ViT primarily serves as a feature extractor and a separate prediction head functions as the generator. Consequently, directly transferring linear attention adaptation paradigms from LLMs to ViTs leads to a substantial performance drop. We attribute this to divergent error propagation: while LLM errors accumulate temporally, ViT errors accumulate spatially and hierarchically. This distorts the global semantic manifold essential for dense prediction, making feature alignment non-negotiable to preserve the spatial consistency vision tasks require.

To address these challenges, we introduce **ViT-AdaLA** (*Adapting Vision Transformers with Linear Attention*). ViT-AdaLA consists of three stages designed to inherit knowledge from a pretrained softmax-based ViT and transfer it to downstream tasks: attention alignment, feature alignment, and supervised fine-tuning. To effectively adapt the prior knowledge from the VFMs, we first align the linear attention module with the original softmax attention in each transformer block. We find that *tuning the vanilla linear attention module yields a strong approximation to the original softmax attention*, outperforming other linear attention variants (Fig. 5 and 8). Although the

linear attention modules are aligned independently in each block during Stage 1, the residual approximation error accumulates across layers. To mitigate this accumulated error, we introduce a feature alignment stage that finetunes the entire linearized model. Specifically, we replace the original softmax attention with the aligned linear attention in Stage 1, and finetune the full linearized ViT to align its final-layer features with those of the frozen softmax-based teacher model. Interestingly, we observe that *the attention alignment in Stage 1 can accelerate convergence during this feature alignment process*. Finally, we perform supervised fine-tuning to transfer the adapted prior knowledge to downstream tasks. Our contributions are three-fold:

- We introduce a new paradigm for ViTs with linear attention that shifts the focus from designing more accurate attention approximations to adapting prior knowledge from pretrained ViTs. Our paradigm enables linearized ViTs to inherit the power of existing VFMs, eliminating the need for expensive training from scratch.
- We introduce *ViT-AdaLA*, which adapts VFMs via attention alignment, feature alignment, and supervised fine-tuning. This progressive alignment allows linear attention models to inherit the strong priors of softmax-based ViTs. Furthermore, our framework is architecture-agnostic and compatible with other linear attention methods.
- We perform extensive experiments on classification and segmentation tasks across multiple VFMs, and compare against a wide range of state-of-the-art linear attention baselines. Experimental results validate the effectiveness, efficiency, and scalability in resolution of ViT-AdaLA across different VFMs and downstream tasks.

2. Related Work

Efficient Attention. The Transformer architecture (Vaswani et al., 2017) has been widely adopted in both natural language processing and vision tasks due to its scalability. However, the quadratic complexity of standard attention limits long-context understanding, leading to numerous approaches to reduce *memory* and *computation* overhead.

FlashAttention (Dao et al., 2022b; Dao, 2023; Shah et al., 2024) improves memory efficiency by employing tile-based computation instead of explicitly materializing the full attention matrix. To further reduce the number of visual tokens and improve computational efficiency, some methods either select informative tokens (Rao et al., 2021) or merge redundant ones (Bolya et al., 2023; Zeng et al., 2022; Li et al., 2025a). Others propose to distill knowledge from a large ViT to a smaller one (Xiong et al., 2024; Touvron et al., 2021) or a more efficient model (Bick et al., 2025; Wei & Chellappa, 2025). Swin Transformer (Liu et al., 2021; 2022)

introduces a shifted-window mechanism to restrict dense attention computation within local regions. More recently, Mamba-based architectures (Gu & Dao, 2023; Liu et al., 2024; Zhu et al., 2024; Wang et al., 2025) have drawn significant attention due to their linear complexity, achieved through selective state-space modeling. Notably, Mamba can be seen as a variant of linear attention with specialized linear attention and modified block design (Han et al., 2024b).

Linear Attention. Existing linearized Transformers can be broadly categorized into two streams: training-from-scratch-based and linearization-based approaches. Training-from-scratch-based approach targets at designing accurate attention approximation methods and trains from scratch to obtain prior knowledge. One stream designs alternative activation functions after queries and keys for better approximation (Han et al., 2024a; Katharopoulos et al., 2020; Han et al., 2023; Shen et al., 2021; Qin et al., 2022; Bolya et al., 2022; Koohpayegani & Pirsiavash, 2024; Ahmed et al., 2025; Bolya et al., 2022). Another family of methods employs low-rank decomposition to approximate, treating the softmax operation over queries and keys as a whole and decomposing it to derive more effective feature maps (Xiong et al., 2021; Han et al., 2022; Wu et al., 2024; Yaras et al., 2025; Xu et al., 2024). Recent work (Fan et al., 2025) observes that rank augmentation is beneficial for improving the performance. Another stream tries to combine convolution kernel with linear attention, preserving local and global information (Zhou et al., 2025; Cai et al., 2023). However, these methods typically require large-scale pretraining before fine-tuning on downstream tasks, which is computationally and resource intensive.

In contrast, linearization-based approaches aim to adapt existing softmax-based Transformers to linearized one. Hedgehog (Zhang et al., 2024) approximates the attention matrix using the Hedgehog linear-attention module. LoLCATS (Zhang et al., 2025) introduces attention transfer to approximate attention outputs and employs low-rank linearization based on LoRA (Hu et al., 2022) for decoder-based LLMs. Building upon LoLCATS, Lizard (Van Nguyen et al., 2025), a hybrid attention paradigm, combines global attention via GLA (Yang et al., 2024) with local attention. Nevertheless, these methods cannot be directly applied to vision tasks due to architectural differences, as illustrated in Fig. 2. To address this challenge, we propose **ViT-AdaLA**, a novel method to extend the linearization paradigm to ViTs.

3. Method

3.1. Preliminary

First, we briefly review the fundamentals of softmax and linear attention.

Softmax attention. Softmax attention is the fundamental module of the original Transformer, responsible for computing the pairwise attention among all input tokens. Let $\mathbf{X} \in \mathbb{R}^{N \times D}$ denote a sequence of N tokens, each with dimension D . The output $\mathbf{O} \in \mathbb{R}^{N \times D}$ is given by

$$\mathbf{O}_i = \sum_{j=1}^N \frac{\exp(\mathbf{Q}_i \mathbf{K}_j^T)}{\sum_{k=1}^N \exp(\mathbf{Q}_i \mathbf{K}_k^T)} \mathbf{V}_j, \quad (1)$$

where \mathbf{Q} , \mathbf{K} , and \mathbf{V} denote the query, key, and value representations of the input tokens, obtained by multiplying \mathbf{X} with the corresponding projection matrices \mathbf{W}_Q , \mathbf{W}_K , and \mathbf{W}_V , respectively. Here, $\exp(\cdot)$ denotes the exponential function, and we omit the common scaling factor $1/\sqrt{D}$ for simplicity. The computational complexity of softmax attention is $\mathcal{O}(N^2 D)$.

Linear Attention. The kernel trick, expressed as $\exp(\mathbf{Q}\mathbf{K}^T) = \phi(\mathbf{Q})\phi(\mathbf{K}^T)$, is employed to decompose the multiplication of \mathbf{Q} and \mathbf{K} and to reorder the computation:

$$\begin{aligned} \mathbf{O}_i &= \sum_{j=1}^N \frac{\phi(\mathbf{Q}_i)\phi(\mathbf{K}_j^T)}{\sum_{k=1}^N \phi(\mathbf{Q}_i)\phi(\mathbf{K}_k^T)} \mathbf{V}_j, \\ &= \frac{\phi(\mathbf{Q}_i) \sum_{j=1}^N \phi(\mathbf{K}_j^T) \mathbf{V}_j}{\phi(\mathbf{Q}_i) \sum_{k=1}^N \phi(\mathbf{K}_k^T)}, \end{aligned} \quad (2)$$

where $\phi(\cdot) = \text{ELU}(\cdot) + 1$, $\text{ELU}(\cdot)$ indicates the exponential linear unit (Clevert et al., 2015). We also compare with other types in the App. A.3. By reordering the multiplication computation of \mathbf{Q} and \mathbf{K} , linear attention can achieve a computational complexity of $\mathcal{O}(ND^2)$.

3.2. ViT-AdaLA

ViT-AdaLA consists of three stages (see Fig. 4): attention alignment, feature alignment, and supervised fine-tuning.

Stage 1: Attention Alignment. To preserve the original attention quality while approximating softmax attention, we introduce an additional linear attention module and align it with the corresponding softmax attention module. Rather than adapting the linear attention module from scratch, we adapt it from an existing softmax attention module (based on Eq. 2) by simply modifying the computation order of queries, keys, and values using kernel trick. All components of the original model are frozen, except for the added linear attention module, where we only update the three projection matrices \mathbf{W}_Q , \mathbf{W}_K , and \mathbf{W}_V .

Formally, let the input to the i -th block after the first layer normalization be denoted as $\mathbf{O}_i \in \mathbb{R}^{N \times D}$. The output of the original self-attention module is $\mathbf{O}_i = f_{\theta}^{SA}(\mathbf{X}_i) \in \mathbb{R}^{N \times D}$, where $f_{\theta}^{SA}(\cdot)$ denotes the softmax-based self-attention. The

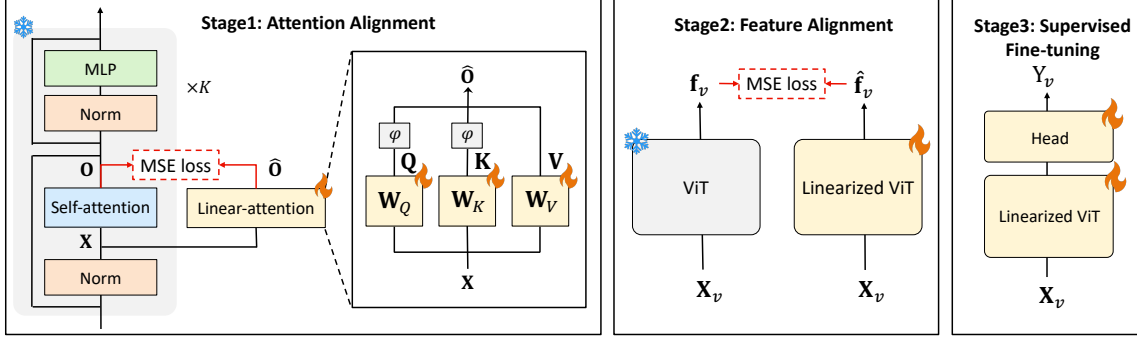


Figure 4. ViT-AdaLA consists of three stages: attention alignment, feature alignment, and supervised fine-tuning. First, softmax attention is approximated by tuning only the linear attention modules. Second, to mitigate residual approximation errors that accumulate across layers, the feature alignment stage finetunes the entire linearized model by aligning its final-layer representations with those of the original softmax-based teacher. Finally, supervised fine-tuning is performed to transfer the adapted prior knowledge to downstream tasks.

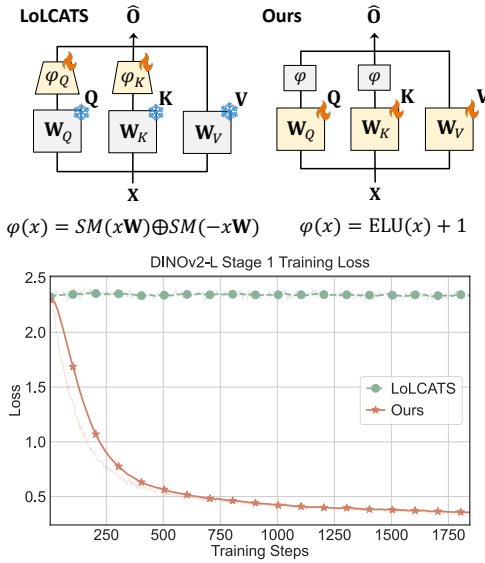


Figure 5. Linear attention architecture and Stage 1 training loss comparison with LoLCATS (SM : softmax; \oplus : concatenation). LoLCATS approximates the attention output based on Hedgehog (Zhang et al., 2024) by tuning only two additional mapping modules applied to the queries and keys individually. In contrast, we tune all query, key, and value weights to approximate the attention output, which is both more efficient and more effective than the original LoLCATS approach.

attention alignment loss \mathcal{L}_{att} is then defined as:

$$\mathcal{L}_{att} = \frac{1}{N \cdot D} \sum_{i=1}^K \sum_{n=1}^N \sum_{d=1}^D (\mathbf{o}_i^{nd} - \hat{\mathbf{o}}_i^{nd})^2, \quad (3)$$

where $\hat{\mathbf{O}}_i = f_{\theta}^{LA}(\mathbf{X}_i)$ denotes the output of the linear attention module, n and d index the token and feature dimension, respectively, and K is the number of layers. The alignment loss is defined using the mean-square-error (MSE), which measures the discrepancy between the feature maps produced by the self-attention and linear-attention modules in

each block. Importantly, the original features remain unchanged. We only adjust the linear-attention module to better approximate the behavior of the softmax self-attention.

Unlike the attention transfer strategy in LoLCATS (Zhang et al., 2025), which tunes only two additional mapping modules applied to the queries and keys (*i.e.*, Hedgehog linear attention), we adopt a vanilla linear attention formulation that relies on a simple activation function and directly tunes the query, key, and value projection matrices. We posit that the vanilla linear attention is highly malleable. Unlike sophisticated approximations whose rigid structural priors can “fight” the teacher during distillation, the vanilla attention’s unconstrained nature avoids optimization bottlenecks, allowing it to flexibly learn necessary approximation patterns. As shown in Fig. 5, this design offers two key advantages compared to Hedgehog-based methods: (i) higher computational efficiency, and (ii) improved approximation quality.

Stage 2: Feature Alignment. Although we align the linear attention module with the softmax-based self-attention in each transformer block, the original features remain untuned, and replacing self-attention with linear attention introduces residual approximation errors to accumulate across blocks (see Fig. 14 in App. B). To ensure that the final output features of the linearized ViT remain consistent with the original model, we directly align the final features of the two models. Benefiting from the attention alignment in Stage 1, the linearized ViT converges faster and more effectively transfers prior knowledge from VFMs (see Sec. 4.3.1).

Specifically, we replace all softmax-based self-attention modules with the linear-attention modules obtained in Stage 1, resulting in a linearized ViT. This linearized ViT is then aligned with the frozen original ViT. Given the same input image $\mathbf{X}_v \in \mathbb{R}^{N \times D}$ for both models, we define the feature alignment loss \mathcal{L}_{fa} as follows:

$$\mathcal{L}_{fa} = \frac{\lambda}{N \cdot D} \sum_{n=1}^N \sum_{d=1}^D (\mathbf{f}_v^{nd} - \hat{\mathbf{f}}_v^{nd})^2, \quad (4)$$

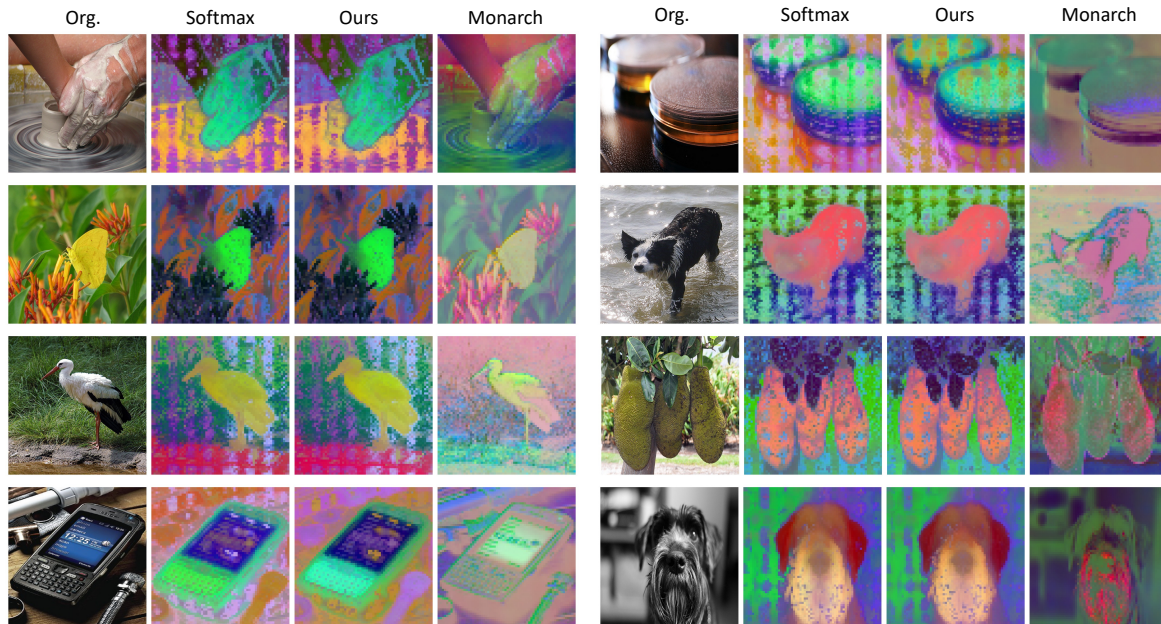


Figure 6. Visualization of PCA-projected features from the final layer of DINOv2-L. We compare the original softmax-based features with those produced by ViT-AdaLA and Monarch attention (Yaras et al., 2025) by projecting them to three channels using PCA. The results indicate that ViT-AdaLA better preserves the prior feature knowledge of the VFM. We provide more visualization results in the App. B.

where $\mathbf{f}_v = \mathcal{F}_{\theta_0}(\mathbf{X}_v)$ and $\hat{\mathbf{f}}_v = \mathcal{F}_{\theta}(\mathbf{X}_v)$ denote the final representations produced by the original ViT and the linearized ViT, respectively. λ controls the scale of the output loss and is set to different values for different VFMs. We utilize MSE loss to align two final features. During this stage, \mathcal{F}_{θ_0} is kept frozen, while only \mathcal{F}_{θ} is updated.

Stage 3: Supervised Fine-tuning. After feature alignment, we transfer the linearized ViT, enriched with prior knowledge from VFMs, to downstream tasks by fine-tuning it on task-specific datasets. In this stage, a task-specific head is appended to the linearized ViT and both the backbone and the task head are updated during this process.

4. Experiment

We first pretrain linearized VFMs using our ViT-AdaLA pipeline through Stages 1 and 2. Specifically, we train four linearized VFMs within the PyTorch Lightning framework using $8 \times$ H100 GPUs. Stage 1 training is conducted on COCO (Lin et al., 2014) for 4 epochs with batch size 32 per GPU, while Stage 2 training is performed on ImageNet-22K (Deng et al., 2009) for 10 to 30 epochs with batch size 16 per GPU. We employ the AdamW optimizer with fixed learning rate $1e^{-2}$ and initial learning rate $1e^{-4}$ and a linearly decaying learning rate schedule for Stage 2. We multiply the learning rate with the ratio of 0.1 to the backbone when training. All models are trained using 512×512 input images, with random cropping and color jitter applied for data augmentation. More details can refer to App. A.1.

After pretraining, we benchmark performance on classification and semantic segmentation against existing linear attention baselines. Additionally, we perform ablation studies to analyze the impact of each training stage.

4.1. Comparison on Classification

Experimental setup. We conduct experiments on the ImageNet-1K (Deng et al., 2009) dataset. We report top-1 accuracy, parameter, throughput, and GFLOPs in Tab. 1. Throughput and peak memory (batch size 1) are measured on a single H100 GPU. This measurement setup extends to Tables 2 and 4. The baselines are constructed by replacing softmax attention modules with their linear counterparts. Full training details are provided in the App. A.1.

Result analysis. Tab. 1 shows that ViT-AdaLA achieves the highest top-1 accuracy among VFMs, *maintaining accuracy within 1% of the original softmax backbone while preserving efficiency*. We can also observe that for decoder-based linearization methods like Hedgehog (Zhang et al., 2024) and LoLCATS (Zhang et al., 2025), the final performance drops significantly since the linearized ViT has not been fully aligned with the VFM backbone, and *aligning attention alone is insufficient to transfer adequate prior knowledge*. This demonstrates that:

For vision models, it is essential to align the final feature representations with the original VFM backbone teacher to ensure effective knowledge transfer.

Table 1. Top-1 fine-tuning accuracy comparison on ImageNet-1K under different vision foundation models with multiple linear attention baselines. We reproduce all baselines to ensure a fair comparison. The classification head is a single linear layer for all the methods.

	Backbone	Res.	Params (M)	FLOPS (G)	Peak Mem. (GB)	Throughput (imgs/s)	Top-1 Acc. (%)
Softmax (Oquab et al., 2024)	DINOv2-L	512 ²	304.20	310.60	1.3181	36.52	86.8
Hedgehog (Zhang et al., 2024)	DINOv2-L	512 ²	305.77	265.41 ↓14.5%	1.2221 ↓7.3%	37.44 ↑2.5%	58.8
LoLCATS (Zhang et al., 2025)	DINOv2-L	512 ²	305.77	265.41 ↓14.5%	1.2221 ↓7.3%	37.44 ↑2.5%	61.6
Linformer (Wang et al., 2020)	DINOv2-L	512 ²	305.77	262.19 ↓15.6%	1.2221 ↓7.3%	45.41 ↑25.3%	68.9
Performer (Choromanski et al., 2021)	DINOv2-L	512 ²	304.20	265.41 ↓14.6%	1.2164 ↓7.7%	36.48 ↑0.1%	75.2
Cosformer (Qin et al., 2022)	DINOv2-L	512 ²	304.20	265.41 ↓14.6%	1.2226 ↓7.2%	39.55 ↑8.2%	75.1
Nyströmformer (Xiong et al., 2021)	DINOv2-L	512 ²	304.20	265.20 ↓14.6%	1.2163 ↓7.7%	18.29 ↓50.8%	82.4
Monarch (Yaras et al., 2025)	DINOv2-L	512 ²	304.20	269.44 ↓13.3%	1.2304 ↓6.7%	18.31 ↓48.9%	82.7
ViT-AdaLA (Stage 2)	DINOv2-L	512 ²	304.20	262.19 ↓15.6%	1.2163 ↓7.7%	41.56 ↑16.1%	84.5
ViT-AdaLA (Ours)	DINOv2-L	512 ²	304.20	262.19 ↓15.6%	1.2163 ↓7.7%	41.56 ↑16.1%	86.0
Softmax (Radford et al., 2021)	CLIP-L	512 ²	304.15	310.60	1.3179	36.82	86.4
ViT-AdaLA (Stage 2)	CLIP-L	512 ²	304.15	262.19 ↓15.6%	1.2161 ↓7.4%	42.14 ↑15.7%	83.4
ViT-AdaLA (Ours)	CLIP-L	512 ²	304.15	262.19 ↓15.6%	1.2161 ↓7.4%	42.14 ↑15.7%	85.5
Softmax (Zhai et al., 2023)	SigLIP-L	512 ²	316.74	312.46	1.3636	40.86	86.9
ViT-AdaLA (Stage 2)	SigLIP-L	512 ²	316.74	264.04 ↓15.5%	1.2620 ↓7.4%	46.91 ↑13.9%	84.9
ViT-AdaLA (Ours)	SigLIP-L	512 ²	316.74	264.04 ↓15.5%	1.2620 ↓7.4%	46.91 ↑13.9%	86.4

For training-from-scratch methods, low-rank approximation yields better than activation-based techniques. However, they incur greater memory and computation due to the mathematical complexity required for high-quality approximation. Nevertheless, these methods still fail to match the performance of ViT-AdaLA or even its Stage 2 baseline. This indicates: *linearization is superior to training-from-scratch methods for extracting prior knowledge from VFMs.*

4.2. Comparison on Semantic Segmentation

Experimental setup. We further conduct experiments on ADE20K (Zhou et al., 2017) and Cityscapes (Cordts et al., 2016) to provide a more fine-grained evaluation of ViT-AdaLA when transferring from VFMs. For both semantic segmentation datasets, we employ the Mask2Former head (Cheng et al., 2022) across all baselines. We consider two experimental settings: evaluating different VFMs on ADE20K in Tab. 2, and assessing the impact of input resolutions on Cityscapes in Tab. 4.

Result analysis. Since segmentation requires more low-level and fine-grained features than classification, the ability of linearization to extract robust prior knowledge is essential for maintaining high performance in dense prediction tasks. As shown in Tab. 2, ViT-AdaLA demonstrates strong performance across various VFMs, rivaling even supervised baselines such as the IN1K-pretrained ViT (Dosovitskiy et al., 2020) This highlights *the generalizability of ViT-AdaLA in effectively distilling prior knowledge from diverse VFMs and transferring it to different downstream tasks.*

We further explore the scaling ability of our ViT-AdaLA for higher resolution images as shown in Tab. 4. Our linear

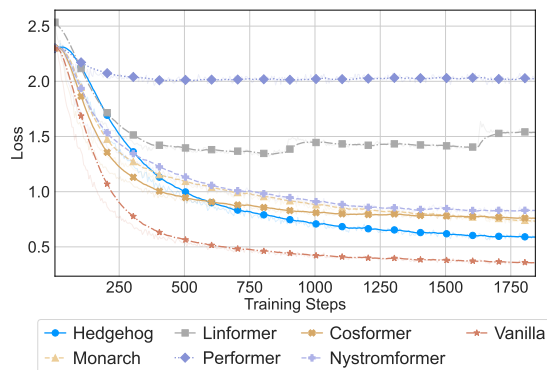


Figure 8. Training loss comparison of different linear attention variants in Stage 1 on DINOv2-L. To ensure a fair comparison, the query, key, and value weights are tuned in every layer for each baseline. Vanilla linear attention exhibits superior approximation performance compared to the other variants.

approach overcomes the efficiency bottleneck of softmax attention, delivering >50% memory savings and 2× faster inference. Moreover, ViT-AdaLA generalizes well across scales: although distilled at a resolution of 512², its performance improves from 72.40% to 78.73% when scaled up to 1024², which shows the following property:

ViT-AdaLA can scale to higher-resolution images, even when pretrained on lower-resolution ones.

Such a property enables more efficient pretraining and broader applications of ViT-AdaLA. Ultimately, this flexibility resolves the tension between training costs and inference quality, establishing ViT-AdaLA as a versatile and practical paradigm for large-resolution dense prediction tasks.

Table 2. mIoU fine-tuning comparison on ADE20K under different vision foundation models with multiple linear attention baselines. We reproduce all baselines to ensure a fair comparison. The segmentation head is Mask2former for all the methods.

	Backbone	Res.	Params (M)	FLOPS (G)	Peak Mem. (GB)	Throughput (imgs/s)	mIoU (%)
Softmax (Oquab et al., 2024)	DINOv2-L	512 ²	304.20	310.60	1.3181	36.52	56.73
Hedgehog (Zhang et al., 2024)	DINOv2-L	512 ²	305.77	265.41 \downarrow 14.5%	1.2221 \downarrow 7.3%	37.44 \uparrow 2.5%	22.52
LoLCATS (Zhang et al., 2025)	DINOv2-L	512 ²	305.77	265.41 \downarrow 14.5%	1.2221 \downarrow 7.3%	37.44 \uparrow 2.5%	17.42
Linformer (Wang et al., 2020)	DINOv2-L	512 ²	305.77	262.19 \downarrow 15.6%	1.2221 \downarrow 7.3%	45.41 \uparrow 25.3%	18.82
Performer (Choromanski et al., 2021)	DINOv2-L	512 ²	304.20	265.41 \downarrow 14.6%	1.2164 \downarrow 7.7%	36.48 \uparrow 0.1%	41.16
Cosformer (Qin et al., 2022)	DINOv2-L	512 ²	304.20	265.41 \downarrow 14.6%	1.2226 \downarrow 7.2%	39.55 \uparrow 8.2%	27.17
Nyströmformer (Xiong et al., 2021)	DINOv2-L	512 ²	304.20	265.20 \downarrow 14.6%	1.2163 \downarrow 7.7%	18.29 \downarrow 50.8%	41.16
Monarch (Yaras et al., 2025)	DINOv2-L	512 ²	304.20	269.44 \downarrow 13.3%	1.2304 \downarrow 6.7%	18.31 \downarrow 48.9%	44.95
ViT-AdaLA (Stage 2)	DINOv2-L	512 ²	304.20	262.19 \downarrow 15.6%	1.2163 \downarrow 7.7%	41.56 \uparrow 16.1%	52.46
ViT-AdaLA (Ours)	DINOv2-L	512 ²	304.20	262.19 \downarrow 15.6%	1.2163 \downarrow 7.7%	41.56 \uparrow 16.1%	55.55
Softmax (Zhai et al., 2023)	SigLIP-L	512 ²	316.74	312.46	1.3636	41.05	54.4
ViT-AdaLA (Stage 2)	SigLIP-L	512 ²	316.74	264.04 \downarrow 15.5%	1.2620 \downarrow 7.4%	47.05 \uparrow 14.6%	51.39
ViT-AdaLA (Ours)	SigLIP-L	512 ²	316.74	264.04 \downarrow 15.5%	1.2620 \downarrow 7.4%	47.05 \uparrow 14.6%	53.16
Softmax	IN1K ViT-L	512 ²	304.15	310.60	1.3179	36.47	50.83
ViT-AdaLA (Stage 2)	IN1K ViT-L	512 ²	304.15	262.19 \downarrow 15.6%	1.2161 \downarrow 7.7%	42.56 \uparrow 16.7%	46.92
ViT-AdaLA (Ours)	IN1K ViT-L	512 ²	304.15	262.19 \downarrow 15.6%	1.2161 \downarrow 7.7%	42.56 \uparrow 16.7%	49.75

Table 3. Ablation study of Stages 1 and 2 training using DINOv2-L, evaluated on the ADE20K dataset.

Stage 1	Stage 2	mIoU
×	×	22.92
✓	×	19.37
×	✓	52.46
✓	✓	55.55
Softmax		56.73

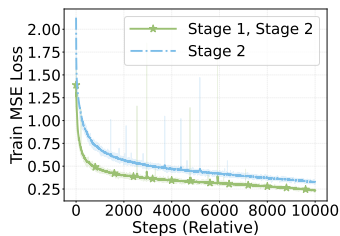


Figure 7. Stage 2 loss comparison between with and without Stage 1 initialization.

4.3. Ablation Study

We provide ablations below to explore the effectiveness of pretraining stages, the scalability of various image sizes and the adaptation of the task model.

4.3.1. EFFECTIVENESS OF PRETRAINING STAGES

The effectiveness of Stage 1. As shown in Tab. 3, Stage 1 initialization can benefit the Stage 2 performance, which will lead to a better performance on dense prediction tasks. To investigate the influence of Stage 1 to Stage 2, we compare the Stage 2 training loss with and without the Stage 1 pretraining in Fig. 7, which indicates that:

Stage 1 accelerates Stage 2 convergence and enhances prior knowledge extraction from the VFM teacher.

We further evaluate alternative linear attention mechanisms during the Stage 1 training (see Fig. 8). The results demonstrate that the *vanilla linear attention provides a superior approximation of the original softmax attention compared to other variants*, while retaining high computational effi-

ciency. Notably, *ViT-AdaLA is independent of the specific linear attention architecture used*. Consequently, our framework serves as a flexible foundation for future research into designing efficient and effective linear attention methods.

The effectiveness of Stage 2. We also provide extensive experiments to validate the effectiveness of Stage 2 on classification and segmentation in Tables 1-4.

From these results, we can see that Stage 2 plays a significant role in our training paradigm. This stage can inherit most of the prior knowledge from VFMs by aligning the final layer representations, which is effective in transferring to different downstream tasks. Fig. 10 illustrates the dynamic perfor-

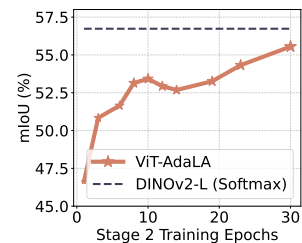


Figure 10. ADE20K performance across different Stage 2 training epochs for DINOv2-L.

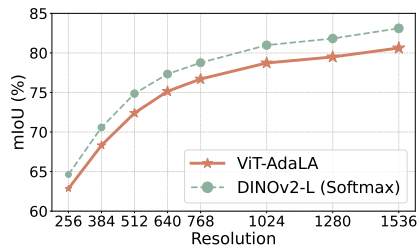
It is evident that ViT-AdaLA effectively extracts prior knowledge within the first few epochs, and performance continues to increase as training progresses. However, we observe that the performance eventually saturates after reaching a peak. Consequently, we adopt an early stopping strategy for Stage 2.

4.3.2. RESOLUTION SCALABILITY ANALYSIS

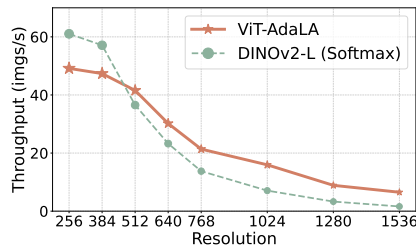
To demonstrate the scaling property and the efficiency of ViT-AdaLA across different resolutions compared to the original model, we present this comparison in Fig. 9. The results indicate that *our ViT-AdaLA can scale to different resolution images (from 256² to 1536²) even pretrained on images with a fixed resolution (512²)*. Moreover, the results

Table 4. mIoU fine-tuning comparison on Cityscapes under different input resolutions (512 vs. 1024) based on DINOv2-L. We reproduce all baselines to ensure a fair comparison. The segmentation head is Mask2former for all the methods.

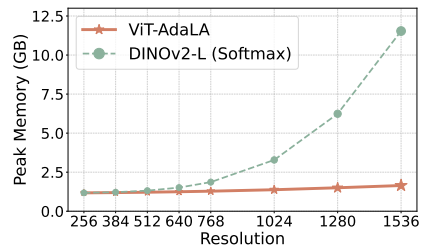
	Backbone	Res.	Params (M)	FLOPS (G)	Peak Mem. (GB)	Throughput (imgs/s)	mIoU (%)
Softmax (Oquab et al., 2024)	DINOv2-L	512 ²	304.20	310.60	1.3181	36.52	74.86
Hedgehog (Zhang et al., 2024)	DINOv2-L	512 ²	305.77	265.41 _{↓14.5%}	1.2221 _{↓7.3%}	37.44 _{↑2.5%}	43.97
LoLCATS (Zhang et al., 2025)	DINOv2-L	512 ²	305.77	265.41 _{↓14.5%}	1.2221 _{↓7.3%}	37.44 _{↑2.5%}	34.71
Linformer (Wang et al., 2020)	DINOv2-L	512 ²	305.77	262.19 _{↓15.6%}	1.2221 _{↓7.3%}	45.41 _{↑25.3%}	37.24
Performer (Choromanski et al., 2021)	DINOv2-L	512 ²	304.20	265.41 _{↓14.6%}	1.2164 _{↓7.7%}	36.48 _{↑0.1%}	43.11
Cosformer (Qin et al., 2022)	DINOv2-L	512 ²	304.20	265.41 _{↓14.6%}	1.2226 _{↓7.2%}	39.55 _{↑8.2%}	44.52
Nyströmformer (Xiong et al., 2021)	DINOv2-L	512 ²	304.20	265.20 _{↓14.6%}	1.2163 _{↓7.7%}	18.29 _{↓50.8%}	48.97
Monarch (Yaras et al., 2025)	DINOv2-L	512 ²	304.20	269.44 _{↓13.3%}	1.2304 _{↓6.7%}	18.31 _{↓48.9%}	50.84
ViT-AdaLA (Stage 2)	DINOv2-L	512 ²	304.20	262.19 _{↓15.6%}	1.2163 _{↓7.7%}	41.56 _{↑16.1%}	71.32
ViT-AdaLA (Ours)	DINOv2-L	512 ²	304.20	262.19 _{↓15.6%}	1.2163 _{↓7.7%}	41.56 _{↑16.1%}	72.40
Softmax (Oquab et al., 2024)	DINOv2-L	1024 ²	304.20	1241.0	3.2836	7.07	80.98
Hedgehog (Zhang et al., 2024)	DINOv2-L	1024 ²	305.77	442.24 _{↓64.4%}	1.3823 _{↓57.9%}	15.38 _{↑117.4%}	44.17
LoLCATS (Zhang et al., 2025)	DINOv2-L	1024 ²	305.77	442.24 _{↓64.4%}	1.3823 _{↓57.9%}	15.38 _{↑117.4%}	33.66
Linformer (Wang et al., 2020)	DINOv2-L	1024 ²	305.77	429.35 _{↓65.4%}	1.3999 _{↓57.4%}	17.83 _{↑152.0%}	26.63
Performer (Choromanski et al., 2021)	DINOv2-L	1024 ²	304.20	442.24 _{↓64.4%}	1.3765 _{↓58.1%}	15.23 _{↑115.3%}	42.58
Cosformer (Qin et al., 2022)	DINOv2-L	1024 ²	304.20	442.24 _{↓64.4%}	1.3945 _{↓57.5%}	15.29 _{↑116.1%}	44.50
Nyströmformer (Xiong et al., 2021)	DINOv2-L	1024 ²	304.20	442.24 _{↓64.4%}	1.3764 _{↓58.1%}	14.61 _{↑106.5%}	47.56
Monarch (Yaras et al., 2025)	DINOv2-L	1024 ²	304.20	500.24 _{↓59.7%}	1.5469 _{↓52.9%}	9.74 _{↑37.6%}	55.18
ViT-AdaLA (Stage 2)	DINOv2-L	1024 ²	304.20	429.35 _{↓65.4%}	1.3764 _{↓58.1%}	15.95 _{↑125.4%}	77.53
ViT-AdaLA (Ours)	DINOv2-L	1024 ²	304.20	429.35 _{↓65.4%}	1.3764 _{↓58.1%}	15.95 _{↑125.4%}	78.73



(a) mIoU



(b) Throughput



(c) Peak memory (single image evaluation)

Figure 9. Resolution scalability analysis on the Cityscapes dataset in terms of (a) mIoU, (b) throughput, and (c) peak memory.

also show that our method can reach a close performance to DINOv2-L while keeping efficient to larger solutions. It is worth noting that standard softmax attention $\mathcal{O}(N^2D)$ can be more efficient than linear attention $\mathcal{O}(ND^2)$ when the sequence length N is smaller than the head dimension D , e.g., $N = 256$ and $D = 1024$.

4.3.3. DIRECTLY ADAPTING THE TASK MODEL

In addition to VFM adaptation, ViT-AdaLA supports the direct adaptation of downstream task models. Fig. 11 illustrates that this approach slightly outperforms VFM-only adaptation, highlighting the effectiveness of our method in task-specific applications. Unlike the general-purpose VFM, the task model has

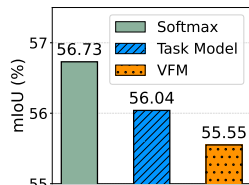


Figure 11. ADE20K performance of adapting the task model or the VFM for DINOv2-L.

already optimized its representations for the target distribution, allowing ViT-AdaLA to inherit more discriminative, task-relevant priors during the linearization process. Consequently, this flexibility ensures that our framework can effectively leverage the best available teacher, whether it is a broad foundation model or a specialized expert.

5. Conclusion

We introduce ViT-AdaLA, a framework that adapts Vision Foundation Model (VFM) priors into linearized ViTs without large-scale pretraining. Our three-stage alignment process effectively distills priors, accelerates convergence, and ensures robust resolution scalability. This paradigm offers a fresh perspective for linearization research, paving the way for high-resolution image applications such as diffusion and 3D generation. Future research can explore more efficient and effective linearization architectures.

Impact Statement

Our work focuses on advancing model efficiency through improved linear attention mechanisms for vision transformers (ViTs). By linearizing existing pretrained ViTs and reducing computational and memory costs, ViT-AdaLA has the potential to lower the barrier to deploying large-scale pretrained vision models with long input sequences in resource-constrained settings, such as edge devices, robotics, and real-time perception systems. This may enable a broader access to advanced visual understanding technologies and support applications in areas including autonomous systems, healthcare imaging, and environmental monitoring.

From the ethical perspective, the techniques presented in this paper do not introduce new modalities of data collection or supervision and rely on publicly available datasets. As a result, the ethical consideration is largely similar to those associated with existing vision foundation models, including potential biases present in pretraining data and downstream misuses in surveillance or privacy-sensitive applications. These risks are not unique to our method but may be amplified if efficient models enable wider deployment. Responsible use, dataset auditing, and appropriate governance remain essential.

Looking forward, we hope our work encourages further research into efficient and adaptable vision models that balance performance, scalability, and responsible deployment. We do not foresee any immediate negative societal impacts arising uniquely from this work beyond those already associated with large-scale visual recognition systems.

References

- Ahmed, S., Li, J., Zhuang, W., Chen, C., and Lyu, L. Mixa: A mixed attention approach with stable lightweight linear attention to enhance efficiency of vision transformers at the edge. In *ICCV*, pp. 21187–21196, 2025.
- Bick, A., Katsch, T., Sohoni, N. S., Desai, A. D., and Gu, A. Llama: Scaling distilled recurrent models for efficient language processing. In *First Workshop on Scalable Optimization for Efficient and Adaptive Foundation Models*, 2025.
- Bolya, D., Fu, C.-Y., Dai, X., Zhang, P., and Hoffman, J. Hydra attention: Efficient attention with many heads. In *ECCV*, pp. 35–49, 2022.
- Bolya, D., Fu, C.-Y., Dai, X., Zhang, P., Feichtenhofer, C., and Hoffman, J. Token merging: Your vit but faster. In *ICLR*, 2023.
- Cai, H., Li, J., Hu, M., Gan, C., and Han, S. Efficientvit: Lightweight multi-scale attention for high-resolution dense prediction. In *ICCV*, pp. 17302–17313, 2023.
- Chen, R., Zhang, H., Liang, S., Li, J., and Cao, X. Less is more: Fewer interpretable region via submodular subset selection. In *ICLR*, 2024.
- Chen, R., Guo, X., Liu, K., Liang, S., Liu, S., Zhang, Q., Zhang, H., and Cao, X. Where mllms attend and what they rely on: Explaining autoregressive token generation. *arXiv preprint arXiv:2509.22496*, 2025a.
- Chen, R., Liang, S., Li, J., Liu, S., Li, M., Huang, Z., Zhang, H., and Cao, X. Interpreting object-level foundation models via visual precision search. In *CVPR*, pp. 30042–30052, 2025b.
- Cheng, B., Misra, I., Schwing, A. G., Kirillov, A., and Girdhar, R. Masked-attention mask transformer for universal image segmentation. In *CVPR*, pp. 1290–1299, 2022.
- Choromanski, K. M., Likhoshesterov, V., Dohan, D., Song, X., Gane, A., Sarlos, T., Hawkins, P., Davis, J. Q., Mohiuddin, A., Kaiser, L., et al. Rethinking attention with performers. In *ICLR*, 2021.
- Clevert, D.-A., Unterthiner, T., and Hochreiter, S. Fast and accurate deep network learning by exponential linear units (elus). *arXiv preprint arXiv:1511.07289*, 4(5):11, 2015.
- Cordts, M., Omran, M., Ramos, S., Rehfeld, T., Enzweiler, M., Benenson, R., Franke, U., Roth, S., and Schiele, B. The cityscapes dataset for semantic urban scene understanding. In *CVPR*, pp. 3213–3223, 2016.
- Dao, T. Flashattention-2: Faster attention with better parallelism and work partitioning. *arXiv preprint arXiv:2307.08691*, 2023.
- Dao, T., Chen, B., Sohoni, N. S., Desai, A., Poli, M., Grogan, J., Liu, A., Rao, A., Rudra, A., and Ré, C. Monarch: Expressive structured matrices for efficient and accurate training. In *ICML*, pp. 4690–4721, 2022a.
- Dao, T., Fu, D., Ermon, S., Rudra, A., and Ré, C. Flashattention: Fast and memory-efficient exact attention with io-awareness. In *NeurIPS*, volume 35, pp. 16344–16359, 2022b.
- Deng, J., Dong, W., Socher, R., Li, L.-J., Li, K., and Fei-Fei, L. Imagenet: A large-scale hierarchical image database. In *CVPR*, pp. 248–255, 2009.
- Devlin, J., Chang, M.-W., Lee, K., and Toutanova, K. Bert: Pre-training of deep bidirectional transformers for language understanding. In *ACL*, pp. 4171–4186, 2019.
- Dosovitskiy, A., Beyer, L., Kolesnikov, A., Weissenborn, D., Zhai, X., Unterthiner, T., Dehghani, M., Minderer, M., Heigold, G., Gelly, S., et al. An image is worth 16x16 words: Transformers for image recognition at scale. In *ICML*, 2020.
- Fan, Q., Huang, H., and He, R. Breaking the low-rank dilemma of linear attention. In *CVPR*, pp. 25271–25280, 2025.
- Glorot, X., Bordes, A., and Bengio, Y. Deep sparse rectifier neural networks. In Gordon, G., Dunson, D., and Dudík, M. (eds.), *AISTAS*, volume 15, pp. 315–323, 11–13 Apr 2011.
- Goldstein, D., Alcaide, E., Lu, J., and Cheah, E. Radlads: Rapid attention distillation to linear attention decoders at scale. *arXiv preprint arXiv:2505.03005*, 2025.
- Gu, A. and Dao, T. Mamba: Linear-time sequence modeling with selective state spaces. *arXiv preprint arXiv:2312.00752*, 2023.
- Han, D., Pan, X., Han, Y., Song, S., and Huang, G. Flatten transformer: Vision transformer using focused linear attention. In *ICCV*, pp. 5961–5971, 2023.

- Han, D., Pu, Y., Xia, Z., Han, Y., Pan, X., Li, X., Lu, J., Song, S., and Huang, G. Bridging the divide: Reconsidering softmax and linear attention. In *NeurIPS*, volume 37, pp. 79221–79245, 2024a.
- Han, D., Wang, Z., Xia, Z., Han, Y., Pu, Y., Ge, C., Song, J., Song, S., Zheng, B., and Huang, G. Demystify mamba in vision: A linear attention perspective. In *NeurIPS*, volume 37, pp. 127181–127203, 2024b.
- Han, J., Zeng, L., Du, L., Ye, X., Ding, W., and Feng, J. Modify self-attention via skeleton decomposition for effective point cloud transformer. In *AAAI*, volume 36, pp. 808–816, 2022.
- Hu, E. J., Shen, Y., Wallis, P., Allen-Zhu, Z., Li, Y., Wang, S., Wang, L., Chen, W., et al. Lora: Low-rank adaptation of large language models. *ICLR*, 1(2):3, 2022.
- Katharopoulos, A., Vyas, A., Pappas, N., and Fleuret, F. Transformers are rnns: Fast autoregressive transformers with linear attention. In *ICML*, pp. 5156–5165, 2020.
- Koohpayegani, S. A. and Pirsaviash, H. Sima: Simple softmax-free attention for vision transformers. In *WACV*, pp. 2607–2617, 2024.
- Lan, D., Sun, W., Hu, J., Du, J., and Cheng, Y. Liger: Linearizing large language models to gated recurrent structures. In *ICML*, 2025.
- Li, Y., Bao, W., Ye, B., Tan, Z., Chen, T., Liu, H., and Kong, Y. Window token concatenation for efficient visual large language models. In *CVPRW*, pp. 3187–3197, 2025a.
- Li, Y., Lai, Z., Bao, W., Tan, Z., Dao, A., Sui, K., Shen, J., Liu, D., Liu, H., and Kong, Y. Visual large language models for generalized and specialized applications. *arXiv preprint arXiv:2501.02765*, 2025b.
- Li, Y., Li, X., Li, T., He, W., Kong, Y., and Ren, L. Vit-split: Unleashing the power of vision foundation models via efficient splitting heads. In *ICCV*, pp. 1979–1989, October 2025c.
- Lin, T.-Y., Maire, M., Belongie, S., Hays, J., Perona, P., Ramanan, D., Dollár, P., and Zitnick, C. L. Microsoft coco: Common objects in context. In *ECCV*, pp. 740–755, 2014.
- Liu, Y., Tian, Y., Zhao, Y., Yu, H., Xie, L., Wang, Y., Ye, Q., Jiao, J., and Liu, Y. Vmamba: Visual state space model. In *NeurIPS*, volume 37, pp. 103031–103063, 2024.
- Liu, Z., Lin, Y., Cao, Y., Hu, H., Wei, Y., Zhang, Z., Lin, S., and Guo, B. Swin transformer: Hierarchical vision transformer using shifted windows. In *ICCV*, pp. 10012–10022, 2021.
- Liu, Z., Hu, H., Lin, Y., Yao, Z., Xie, Z., Wei, Y., Ning, J., Cao, Y., Zhang, Z., Dong, L., et al. Swin transformer v2: Scaling up capacity and resolution. In *CVPR*, pp. 12009–12019, 2022.
- Liu, Z., Kundu, S., Jiang, L., Li, A., Ronanki, S., Bodapati, S., Datta, G., and Beereel, P. A. Lawcat: Efficient distillation from quadratic to linear attention with convolution across tokens for long context modeling. In *EMNLP Findings*, pp. 20865–20881, 2025.
- Oquab, M., Darcet, T., Moutakanni, T., Vo, H., Szafraniec, M., Khalidov, V., Fernandez, P., Haziza, D., Massa, F., El-Nouby, A., et al. Dinov2: Learning robust visual features without supervision. *Transactions on Machine Learning Research Journal*, 2024.
- Qin, Z., Sun, W., Deng, H., Li, D., Wei, Y., Lv, B., Yan, J., Kong, L., and Zhong, Y. cosformer: Rethinking softmax in attention. In *ICLR*, 2022.
- Radford, A., Kim, J. W., Hallacy, C., Ramesh, A., Goh, G., Agarwal, S., Sastry, G., Askell, A., Mishkin, P., Clark, J., et al. Learning transferable visual models from natural language supervision. In *ICML*, pp. 8748–8763, 2021.
- Rao, Y., Zhao, W., Liu, B., Lu, J., Zhou, J., and Hsieh, C.-J. Dynamicvit: Efficient vision transformers with dynamic token sparsification. In *NeurIPS*, volume 34, pp. 13937–13949, 2021.
- Shah, J., Bikshandi, G., Zhang, Y., Thakkar, V., Ramani, P., and Dao, T. Flashattention-3: Fast and accurate attention with asynchrony and low-precision. In *NeurIPS*, volume 37, pp. 68658–68685, 2024.
- Shen, Z., Zhang, M., Zhao, H., Yi, S., and Li, H. Efficient attention: Attention with linear complexities. In *WACV*, pp. 3531–3539, 2021.
- Touvron, H., Cord, M., Douze, M., Massa, F., Sablayrolles, A., and Jégou, H. Training data-efficient image transformers & distillation through attention. In *ICML*, pp. 10347–10357, 2021.
- Van Nguyen, C., Zhang, R., Deilamsalehy, H., Mathur, P., Lai, V. D., Wang, H., Subramanian, J., Rossi, R. A., Bui, T., Vlassis, N., et al. Lizard: An efficient linearization framework for large language models. *arXiv preprint arXiv:2507.09025*, 2025.
- Vaswani, A., Shazeer, N., Parmar, N., Uszkoreit, J., Jones, L., Gomez, A. N., Kaiser, Ł., and Polosukhin, I. Attention is all you need. In *NeurIPS*, volume 30, 2017.
- Wang, F., Yang, T., Yu, Y., Ren, S., Wei, G., Wang, A., Shao, W., Zhou, Y., Yuille, A., and Xie, C. Adventurer: Optimizing vision mamba architecture designs for efficiency. In *CVPR*, pp. 30157–30166, 2025.
- Wang, S. and Zhang, Z. Improving cur matrix decomposition and the nyström approximation via adaptive sampling. *JMLR*, 14(1):2729–2769, 2013.
- Wang, S., Li, B. Z., Khabsa, M., Fang, H., and Ma, H. Linformer: Self-attention with linear complexity. *arXiv preprint arXiv:2006.04768*, 2020.
- Wei, G. and Chellappa, R. Vit-linearizer: Distilling quadratic knowledge into linear-time vision models. *arXiv preprint arXiv:2504.00037*, 2025.
- Wu, C., Che, M., and Yan, H. The cur decomposition of self-attention matrices in vision transformers. *Authorea Preprints*, 2024.
- Xiong, Y., Zeng, Z., Chakraborty, R., Tan, M., Fung, G., Li, Y., and Singh, V. Nyströmformer: A nyström-based algorithm for approximating self-attention. In *AAAI*, volume 35, pp. 14138–14148, 2021.
- Xiong, Y., Varadarajan, B., Wu, L., Xiang, X., Xiao, F., Zhu, C., Dai, X., Wang, D., Sun, F., Iandola, F., et al. EfficientSAM: Leveraged masked image pretraining for efficient segment anything. In *CVPR*, pp. 16111–16121, 2024.
- Xu, Y., Li, C., Li, D., Sheng, X., Jiang, F., Tian, L., and Barsoum, E. Qt-vit: Improving linear attention in vit with quadratic Taylor expansion. In *NeurIPS*, pp. 83048–83067, 2024.

- Yang, S., Wang, B., Shen, Y., Panda, R., and Kim, Y. Gated linear attention transformers with hardware-efficient training. In *ICML*, 2024.
- Yaras, C., Xu, A. S., Abillama, P., Lee, C., and Balzano, L. Monarchattention: Zero-shot conversion to fast, hardware-aware structured attention. *arXiv preprint arXiv:2505.18698*, 2025.
- Zeng, W., Jin, S., Liu, W., Qian, C., Luo, P., Ouyang, W., and Wang, X. Not all tokens are equal: Human-centric visual analysis via token clustering transformer. In *CVPR*, pp. 11101–11111, 2022.
- Zhai, X., Mustafa, B., Kolesnikov, A., and Beyer, L. Sigmoid loss for language image pre-training. In *ICCV*, pp. 11975–11986, 2023.
- Zhang, M., Bhatia, K., Kumbong, H., and Re, C. The hedgehog & the porcupine: Expressive linear attentions with softmax mimicry. In *ICLR*, 2024.
- Zhang, M., Arora, S., Chalamala, R., Spector, B. F., Wu, A., Ramesh, K., Singhal, A., and Re, C. Lolcats: On low-rank linearizing of large language models. In *ICLR*, 2025.
- Zhou, B., Zhao, H., Puig, X., Fidler, S., Barriuso, A., and Torralba, A. Scene parsing through ade20k dataset. In *CVPR*, pp. 633–641, 2017.
- Zhou, Y., Xu, Q., Cui, J., Zhou, J., Zhang, J., Hong, R., and Zhang, H. Care transformer: Mobile-friendly linear visual transformer via decoupled dual interaction. In *CVPR*, pp. 20135–20145, 2025.
- Zhu, L., Liao, B., Zhang, Q., Wang, X., Liu, W., and Wang, X. Vision mamba: efficient visual representation learning with bidirectional state space model. In *ICML*, pp. 62429–62442, 2024.

A. Experiments

A.1. Configurations of ViT-AdaLA under Different VFMs

We present the hyper-parameter settings for ViT-AdaLA with various VFMs in Table 5.

Table 5. Hyperparameters of different training stages and VFMs.

	Stage 1	Stage 2				Stage 3	
		DINOv2	SigLIP	CLIP	IN-1K	Cls	seg
Epochs	4	30	10	15	20	10	20
Batch size	32	16				8	
Learning rate	1e-2	1e-3				1e-4	
Weight decay	0.05						
Learning schedule	fixed	Polynomial (decay factor of 0.9)					
Optimizer	AdamW						
Datasets	COCO	ImageNet22K			ImageNet1K	ADE20K/Cityscapes	
Heads	N/A	N/A			Linear	Mask2former	
λ	N/A	5	1	4000	1	N/A	

A.2. Details of Compared Baselines

In our experiments, we compare with multiple linear attention baselines including Hedgehog (Zhang et al., 2024), LoLCATS (Zhang et al., 2025), Linformer (Wang et al., 2020), Performer (Choromanski et al., 2021), Cosformer (Qin et al., 2022), Nystromformer (Xiong et al., 2021) and Monarch Attention (Yaras et al., 2025). We reproduce all of these methods according to their perspective publicly available codebase. Below are the details about these baselines:

Hedgehog: Hedgehog (Zhang et al., 2024) proposes two trainable linear attention feature maps $\phi(\cdot)$ after queries and keys. It then learns these two feature maps to mimic standard attention. By employing a distillation loss to train these maps directly against the original attention scores, Hedgehog bridges the performance gap between models. This approach allows the model to maintain linear complexity while recovering most power of the original model.

LoLCATS: LoLCATS (Zhang et al., 2025) adopts a two-stage methodology to linearize LLMs, converting their quadratic complexity attention into a faster, subquadratic form without the massive cost of retraining from scratch. In the first stage, attention transfer, the model utilizes learnable feature maps (inspired by the Hedgehog architecture) trained via the MSE loss to approximate the final attention outputs, rather than the attention matrix itself. The second stage, low-rank adjusting, employs LoRA to tune the Q , K , V , and O projections followed by task-specific supervised fine-tuning. This methodology scales exceptionally well, delivering high performance and efficiency across decoder-based LLMs.

Monarch Attention: Monarch Attention (Yaras et al., 2025) introduces a zero-shot method to convert standard softmax attention into a hardware-efficient, subquadratic form using Monarch matrices. Different from previous methods that require extensive retraining, Monarch Attention allows the plug-and-play replacement of attention layers in pretrained Transformers, maintaining high accuracy. This is achieved by the mathematical property that any dense matrix can be approximated by Monarch matrices (Dao et al., 2022a). By decomposing the attention operation into these structured components, they achieve a complexity of $\mathcal{O}(n\sqrt{n})$. The proposed method proves effective across diverse architectures, including ViTs, various language model configurations (encoder-based and encoder-decoder), and Diffusion Transformers.

Nyströmformer: Nyströmformer (Xiong et al., 2021) proposes to approximate the self-attention using the Nyström method (Wang & Zhang, 2013) by sampling a subset of columns and rows. The core of this method involves a small number of “landmark” points to reconstruct the full, inherently low-rank attention matrix. This method further improves accuracy with

an iterative Moore-Penrose pseudoinverse approximation and residual connections that stabilize training. Nyströmformer allows the model to process sequences with thousands of tokens efficiently while maintaining performance comparable to standard BERT (Devlin et al., 2019) models. In our experiments, we set the number of “landmark” points to 128, which is the head dimension.

Linformer: Linformer (Wang et al., 2020) introduces a low-rank approximation of self-attention based on the empirical observation that attention matrices have low intrinsic rank. It achieves linear complexity by projecting the key and value sequences into a lower-dimensional space using learned projection matrices, reducing the size of the attention computation from $N \times N$ to $N \times k$ with $k \ll N$. These projections are shared across heads and layers, allowing efficient scaling to long sequences with minimal overhead. Experiments show that Linformer matches or closely approaches standard Transformer performance on NLP tasks while dramatically lowering memory and computation costs. In our experiments, we set $k = 32$.

Performer: Performer (Choromanski et al., 2021) rethinks self-attention by replacing the softmax attention kernel with a random feature approximation (FAVOR+), enabling exact linear time attention in expectation. By mapping queries and keys into a positive random feature space, the attention computation is reformulated as a sequence of associative matrix products, avoiding explicit $N \times N$ attention matrices. This design preserve the probabilistic interpretation of softmax attention while strong numerical stability and unbiased estimates. Experiments show that Performer scales effectively to very long sequences with competitive accuracy, though performance depends on the number of random features and can degrade when approximation variance is high.

Cosformer: Cosformer (Qin et al., 2022) revisits the softmax operation in self-attention and proposes replacing it with a cosine-based reweighting mechanism that enables linear-time attention. The authors argue that softmax’s effectiveness comes from two key properties: nonnegativity of the attention matrix and a non-linear reweighting that concentrates attention distributions. Specifically, Cosformer utilizes the ReLU-based kernel to ensure non-negativity and cosine-based reweighting to introduce a “locality bias” that stabilizes training and focuses the model on more relevant local correlations. In experiments, Cosformer evaluates its effectiveness on encoder-based and decoder-based language models.

A.3. Activation Choices for Linear Attention

Fig. 12 shows the influence of activation functions to the Stage 1 loss. Kernel-based linear attention approximation applies a non-negative feature map $\phi(\cdot)$ to the query and key matrices. We compare four different variants, *i.e.*, softmax, softplus, relu and ELU+1.

While linear attention aims to approximate this, the standard self-attention uses the softmax activation to normalize scores:

$$\text{Softmax}(x)_i = \frac{e^{x_i}}{\sum_j e^{x_j}}.$$

In kernelized linear attention, an exponential feature map $\phi(x) = \exp(x)$ is sometimes used to mimic this behavior, though it can be numerically unstable without proper scaling.

ReLU is a popular choice for linear attention due to its computational simplicity and ability to induce sparsity:

$$\phi(x) = \text{ReLU}(x) = \max(0, x).$$

By mapping negative values to zero, it ensures the non-negativity required for the associative property of matrix multiplication in linear attention.

Softplus (Glorot et al., 2011) serves as a smooth, differentiable approximation of the ReLU function: Softplus serves as a smooth, differentiable approximation of the ReLU function:

$$\phi(x) = \text{Softplus}(x) = \ln(1 + e^x).$$

This activation is strictly positive and provides continuous gradients throughout the entire domain, which can lead to more stable training trajectories compared to ReLU. Commonly used in the original linear attention (Katharopoulos et al., 2020), the $\text{ELU}(x) + 1$ feature map ensures that the output is always positive:

$$\phi(x) = \text{ELU}(x) + 1 = \begin{cases} x + 1 & \text{if } x > 0 \\ e^x & \text{if } x \leq 0 \end{cases}.$$

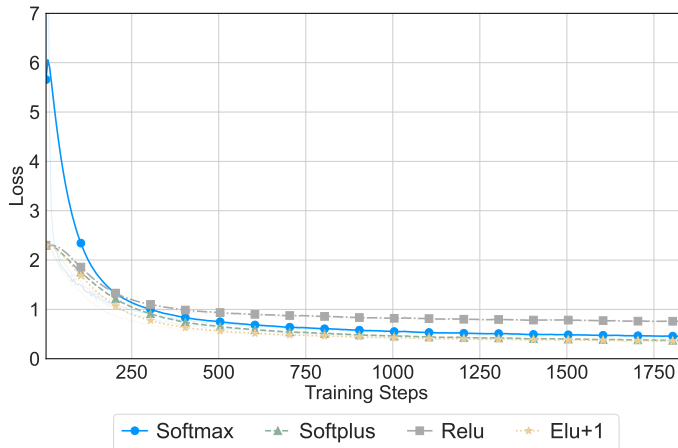


Figure 12. Stage 1 loss comparison across linear-attention activation functions. We compare four activations: softmax, softplus, ReLU, and ELU+1.

This function combines the linear behavior for positive inputs with a smooth exponential decay toward zero for negative inputs.

As illustrated in Fig. 12, ELU + 1 feature map consistently achieves a lower training loss compared to other activation functions. Given its superior convergence characteristics and numerical stability, we select ELU + 1 as the default activation for our final architecture.

A.4. Training Time Comparison

We provide the training time of different VFMs in Stage 1 and Stage 2 in Tab. 6. The result shows that Stage 1 is much faster compared to Stage 2, which indicates the effectiveness and efficiency of the Stage 1.

Table 6. Comparison of training efficiency across various Visual Foundation Models (VFMs) during Stages 1 and 2. Stage 1 is conducted using the COCO dataset, while Stage 2 utilizes ImageNet-22K for large-scale pretraining. All the experiments are conducted on 8 H100s.

Stages	Stage 1 Time (per epoch)	Stage 2 Time (per epoch)
DINOv2-L	4min 37s	10h 48min 46s
SigLIP-L	4min 19s	11h 22min 15s
CLIP-L	5min 56s	11h 09min 21s
IN1K-L	4min 34s	10h 02min 54s
Mean	4min 51s	10h 55min 41s

A.5. Performance on Smaller Size VFMs

Apart from the results on DINOv2-L, we also report experiments on DINOv2-B in Tab. 7 for comparison. The results show that the performance gap between the original softmax model and our ViT-AdaLA is small, demonstrating the effectiveness of our method across different model sizes.

A.6. Comparison with Training-from-Scratch-based Methods

To better highlight the performance and efficiency gap between training-from-scratch baselines and our approach, we train a vanilla linear-attention ViT from scratch on ImageNet-1K for 200 epochs. We then fine-tune it on three downstream datasets and compare it with the softmax baseline and our ViT-AdaLA in Tab. 8. The results show that training-from-scratch linear attention lags substantially behind ViT-AdaLA, suggesting that much longer pretraining may be required to reach competitive accuracy. Overall, these findings demonstrate the effectiveness of our method and its faster convergence in inheriting the prior knowledge from VFMs.

Table 7. Performance comparison using DINOv2-B on ADE20K, Cityscapes and ImageNet-1K. We pretrained our ViT-AdaLA (DINOv2-B) for 40 epochs.

Method	ADE20K (mIoU)	Cityscapes (mIoU)	IN1K (Acc.)
Softmax (DINOv2-B)	53.93	79.73	84.93
ViT-AdaLA (DINOv2-B)	51.46	74.60	84.37

Table 8. Performance comparison of training-from-scratch and on ADE20K, Cityscapes, and IN1K. Our ViT-AdaLA is pretrained for 20 epochs (Stage 2) on ImageNet-22K, whereas the vanilla linear-attention baseline is pretrained from scratch on ImageNet-1K for 200 epochs to ensure a fair comparison.

Method	ADE20K (mIoU)	Cityscapes (mIoU)	IN1K (Acc.)
Softmax (IN1K-L)	50.83	74.86	85.66
ViT-AdaLA (IN1K-L)	49.75	72.40	84.23
Vanilla Linear Attention (train from scratch, IN1K-L)	25.80	45.09	65.72

A.7. Only Tuning the Query, Key and Value Matrices

To investigate the impact of tuning only the query, key, and value (QKV) matrices, we present a comparative analysis in Table 9. We observe a decrease in performance when tuning only the QKV matrices compared to tuning all components. We hypothesize that this drop is caused by overfitting when distilling knowledge from the softmax-based ViT. Specifically, the QKV projections alone may lack the representational capacity to absorb the rich, high-dimensional distributions of the teacher model. By forcing the network to adapt solely through its attention mechanisms, the model distorts its learned feature space, leading to poor generalization. In contrast, updating the MLP blocks alongside the attention mechanisms distributes the distillation signal more evenly.

A.8. Experiments on Classification Tasks

Tab. 10 presents the classification benchmarks for various linear attention models based on CLIP-L. From the results, it can be observed that approximation-based linear attention methods, *i.e.*, Monarch and Nyströmformer, significantly outperform other baselines. This demonstrates that a good approximation of softmax is advantageous. However, these two methods still cannot match the performance of our ViT-AdaLA or even the Stage 2 variant. This performance gap suggests that linearization-based approaches are more effective at distilling prior knowledge from pre-trained VFMs compared to traditional training-from-scratch paradigms.

A.9. Experiments on Segmentation Tasks

Tab. 12 and Tab. 11 present the segmentation results for ADE20K and Cityscapes, respectively. From the results we can see that the overall performance of linear attention baselines have larger gaps with the softmax upper bound compared to the classification results. This is because segmentation requires stronger prior knowledge from the VFMs than the classification tasks do. Despite these challenges, ViT-AdaLA maintains competitive performance with softmax attention, demonstrating its superior ability to extract and preserve critical priors. Furthermore, ViT-AdaLA scales to high-resolution inputs with significant efficiency gains while suffering minimal performance degradation compared to the standard softmax attention.

B. More Visualization Results

Additional PCA visualizations are provided in Figures 13 and 14. Specifically, Figure 13 presents a comparative analysis with Monarch Attention, while Figure 14 illustrates the impact of Stage 1 and Stage 2 through ablation-based PCA results.

Fig. 13 shows that ViT-AdaLA more closely matches the prior features of VFMs than approximation-based linear attention methods such as Monarch, demonstrating its superior ability to distill prior knowledge from softmax-based VFMs. Fig. 14 analyzes the contribution of different stages, showing that Stage 2 effectively preserves most of the original VFM features, while combining both stages yields the strongest retention of prior knowledge.

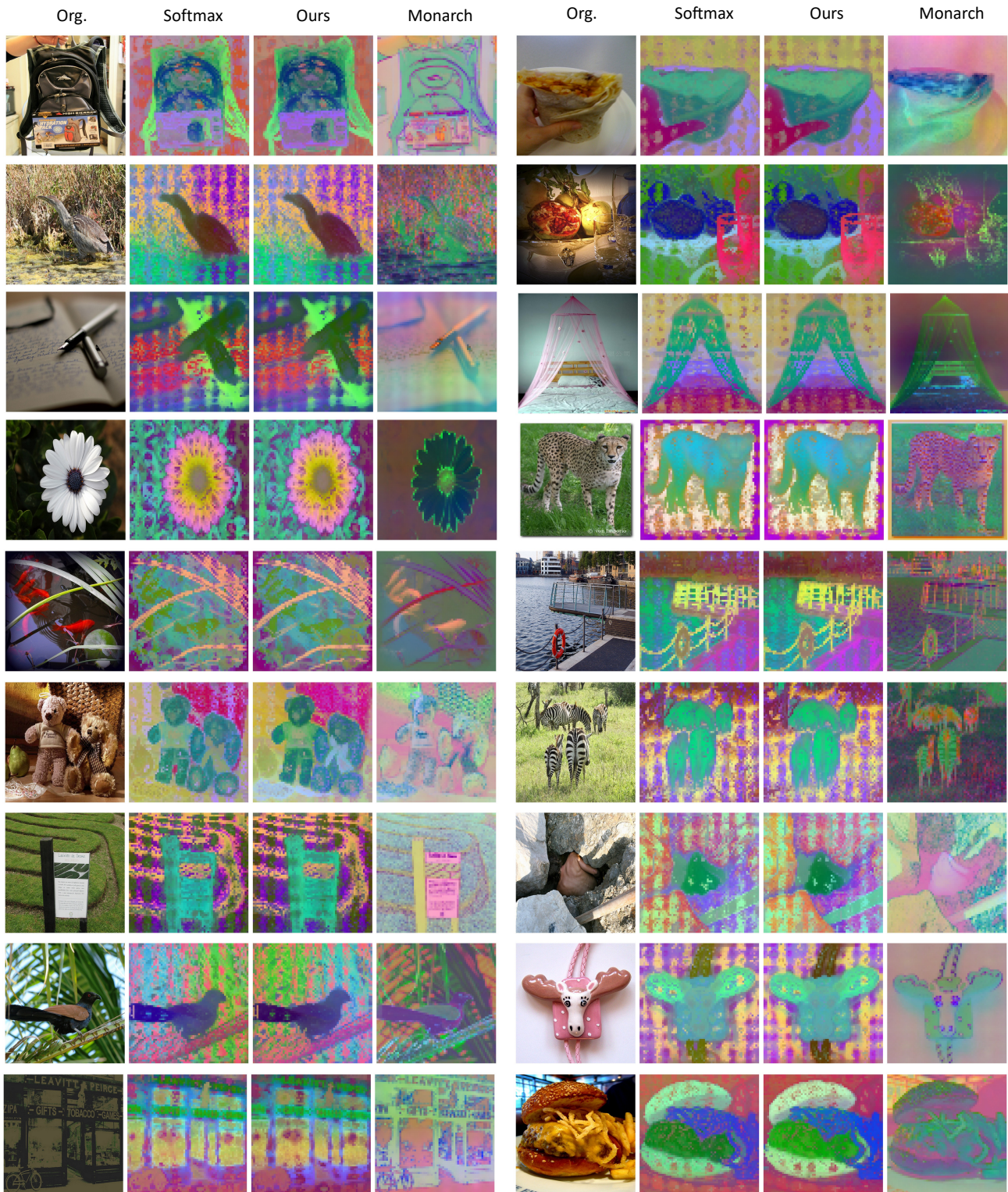


Figure 13. Visualization of PCA-projected features from the final layer of DINOv2-L. Original softmax features, ViT-AdaLA (ours) and Monarch Attention features are compared by projecting to three channels using PCA. These results indicate that ViT-AdaLA can learn more prior knowledge from the original VFM.

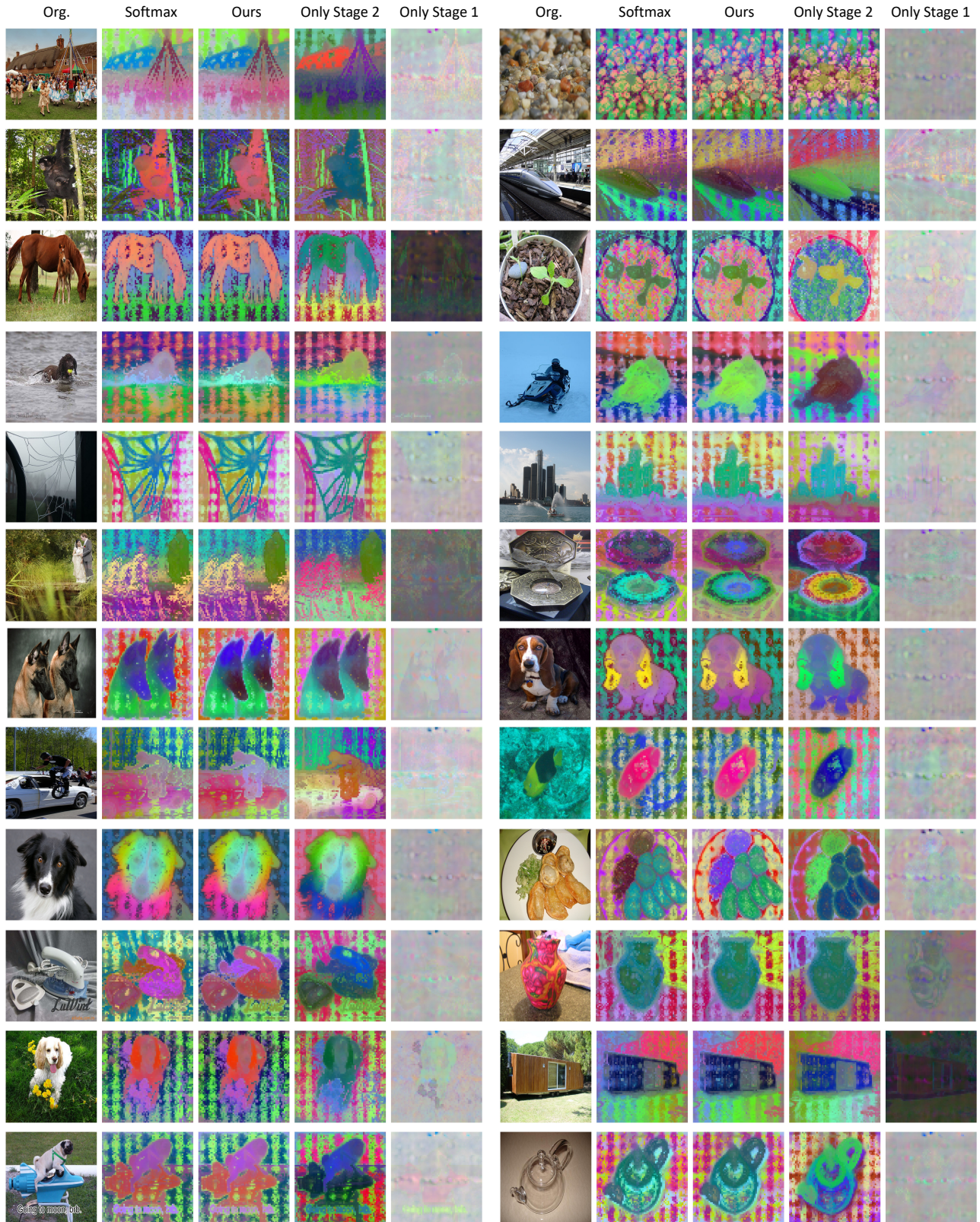


Figure 14. Visualization of PCA-projected features from the final layer of DINOv2-L. We ablate the Stages 1 and 2 training procedures and visualize the resulting PCA features for comparison. The results indicate that Stage 2 is crucial for extracting prior knowledge from VFMs, while the inclusion of Stage 1 further enhances this knowledge transfer.

ViT-AdaLA: Adapting Vision Transformers with Linear Attention

Table 9. Comparison of tuning strategies on CLIP-L and DINOv2-L at 512×512 resolution.

Method	Resolution	Accuracy (IN1K)	mIoU (ADE20K)
CLIP-L (tune all)	512×512	85.5	42.85
CLIP-L (only tune QKV)	512×512	82.5	35.41
DINOv2-L (tune all)	512×512	86.0	55.55
DINOv2-L (only tune QKV)	512×512	76.4	48.82

Table 10. Top-1 fine-tuning accuracy comparison on ImageNet-1K under CLIP-L with multiple linear attention baselines. We reproduce all baselines to ensure a fair comparison. The classification head is a single linear layer for all the methods.

	Backbone	Res.	Params (M)	FLOPS (G)	Peak Mem. (GB)	Throughput (imgs/s)	Top-1 Acc. (%)
Softmax (Oquab et al., 2024)	CLIP-L	512^2	304.20	310.60	1.3181	36.52	86.8
Hedgehog (Zhang et al., 2024)	CLIP-L	512^2	305.77	265.41 \downarrow 14.5%	1.2221 \downarrow 7.3%	37.44 \uparrow 2.5%	67.4
LoLCATS (Zhang et al., 2025)	CLIP-L	512^2	305.77	265.41 \downarrow 14.5%	1.2221 \downarrow 7.3%	37.44 \uparrow 2.5%	67.21
Linformer (Wang et al., 2020)	CLIP-L	512^2	305.77	262.19 \downarrow 15.6%	1.2221 \downarrow 7.3%	45.41 \uparrow 25.3%	56.8
Performer (Choromanski et al., 2021)	CLIP-L	512^2	304.20	265.41 \downarrow 14.6%	1.2164 \downarrow 7.7%	36.48 \uparrow 0.1%	69.9
Cosformer (Qin et al., 2022)	CLIP-L	512^2	304.20	265.41 \downarrow 14.6%	1.2226 \downarrow 7.2%	39.55 \uparrow 8.2%	70.6
Nyströmformer (Xiong et al., 2021)	CLIP-L	512^2	304.20	265.20 \downarrow 14.6%	1.2163 \downarrow 7.7%	18.29 \downarrow 50.8%	80.7
Monarch (Yaras et al., 2025)	CLIP-L	512^2	304.20	269.44 \downarrow 13.3%	1.2304 \downarrow 6.7%	18.31 \downarrow 48.9%	81.5
ViT-AdaLA (Stage 2)	CLIP-L	512^2	304.20	262.19 \downarrow 15.6%	1.2163 \downarrow 7.7%	41.56 \uparrow 16.1%	83.4
ViT-AdaLA (Ours)	CLIP-L	512^2	304.20	262.19 \downarrow 15.6%	1.2163 \downarrow 7.7%	41.56 \uparrow 16.1%	85.5

C. Limitations

Despite the effectiveness of ViT-AdaLA, several limitations remain to be addressed. First, while we have validated our method on classification and segmentation, its generalizability to other downstream tasks, such as object detection and image generation, requires further investigation. Second, although our approach achieves competitive results, a marginal performance gap persists between ViT-AdaLA and full softmax attention in segmentation tasks. Third, the training efficiency of Stage 2 could be enhanced; incorporating advanced distillation strategies, such as masked image modeling, may further accelerate the transfer of prior knowledge. Finally, ViT-AdaLA exhibits increased computational overhead compared to softmax attention when processing low-resolution images. This is a characteristic challenge shared by many linear attention architectures, and developing methods that maintain efficiency across all sequence lengths remains a promising direction for future research.

D. Future Directions

In the future, this linear attention can be extended to vision large language models (VLLMs (Li et al., 2025b)), which process long visual sequences and thus incur substantial computational overhead. By replacing quadratic self-attention with linear variants, these models could achieve significantly improved scalability when handling high-resolution images or long video inputs. Beyond efficiency, this direction also opens up opportunities for better interpretability. For example, integrating explanation methods (Chen et al., 2024; 2025a;b) with linear attention could provide more transparent insights into how visual tokens contribute to model predictions. This is particularly valuable in multimodal settings, where understanding cross-modal interactions remains challenging.

ViT-AdaLA: Adapting Vision Transformers with Linear Attention

Table 11. mIoU fine-tuning comparison on Cityscapes under different input resolutions (512 vs. 1024) based on IN1K ViT-L and SigLIP-L. We reproduce all baselines to ensure a fair comparison. The segmentation head is Mask2former for all the methods.

	Backbone	Res.	Params (M)	FLOPS (G)	Peak Mem. (GB)	Throughput (imgs/s)	mIoU (%)
Softmax (Oquab et al., 2024)	IN1K ViT-L	512 ²	304.15	310.60	1.3181	36.52	65.11
Hedgehog (Zhang et al., 2024)	IN1K ViT-L	512 ²	305.72	265.41 _{↓14.5%}	1.2221 _{↓7.3%}	37.44 _{↑2.5%}	37.69
LoLCATS (Zhang et al., 2025)	IN1K ViT-L	512 ²	305.72	265.41 _{↓14.5%}	1.2221 _{↓7.3%}	37.44 _{↑2.5%}	25.04
Linformer (Wang et al., 2020)	IN1K ViT-L	512 ²	305.72	262.19 _{↓15.6%}	1.2221 _{↓7.3%}	45.41 _{↑25.3%}	17.30
Performer (Choromanski et al., 2021)	IN1K ViT-L	512 ²	304.15	265.41 _{↓14.6%}	1.2164 _{↓7.7%}	36.48 _{↑0.1%}	39.44
Cosformer (Qin et al., 2022)	IN1K ViT-L	512 ²	304.15	265.41 _{↓14.6%}	1.2226 _{↓7.2%}	39.55 _{↑8.2%}	39.33
Nyströmformer (Xiong et al., 2021)	IN1K ViT-L	512 ²	304.15	265.20 _{↓14.6%}	1.2163 _{↓7.7%}	18.29 _{↓50.8%}	45.58
Monarch (Yaras et al., 2025)	IN1K ViT-L	512 ²	304.15	269.44 _{↓13.3%}	1.2304 _{↓6.7%}	18.31 _{↓48.9%}	48.35
ViT-AdaLA (Stage 2)	IN1K ViT-L	512 ²	304.15	262.19 _{↓15.6%}	1.2163 _{↓7.7%}	41.56 _{↑16.1%}	62.24
ViT-AdaLA (Ours)	IN1K ViT-L	512 ²	304.15	262.19 _{↓15.6%}	1.2163 _{↓7.7%}	41.56 _{↑16.1%}	64.16
Softmax (Oquab et al., 2024)	IN1K ViT-L	1024 ²	304.15	1241.0	3.2836	7.07	72.21
Hedgehog (Zhang et al., 2024)	IN1K ViT-L	1024 ²	305.72	442.24 _{↓64.4%}	1.3823 _{↓57.9%}	15.38 _{↑117.4%}	38.07
LoLCATS (Zhang et al., 2025)	IN1K ViT-L	1024 ²	305.72	442.24 _{↓64.4%}	1.3823 _{↓57.9%}	15.38 _{↑117.4%}	25.98
Linformer (Wang et al., 2020)	IN1K ViT-L	1024 ²	305.72	429.35 _{↓65.4%}	1.3999 _{↓57.4%}	17.83 _{↑152.0%}	7.78
Performer (Choromanski et al., 2021)	IN1K ViT-L	1024 ²	304.15	442.24 _{↓64.4%}	1.3765 _{↓58.1%}	15.23 _{↑115.3%}	40.86
Cosformer (Qin et al., 2022)	IN1K ViT-L	1024 ²	304.15	442.24 _{↓64.4%}	1.3945 _{↓57.5%}	15.29 _{↑116.1%}	40.14
Nyströmformer (Xiong et al., 2021)	IN1K ViT-L	1024 ²	304.15	442.24 _{↓64.4%}	1.3764 _{↓58.1%}	14.61 _{↑106.5%}	43.15
Monarch (Yaras et al., 2025)	IN1K ViT-L	1024 ²	304.15	500.24 _{↓59.7%}	1.5469 _{↓52.9%}	9.74 _{↑37.6%}	52.18
ViT-AdaLA (Stage 2)	IN1K ViT-L	1024 ²	304.15	429.35 _{↓65.4%}	1.3764 _{↓58.1%}	15.95 _{↑125.4%}	66.42
ViT-AdaLA (Ours)	IN1K ViT-L	1024 ²	304.15	429.35 _{↓65.4%}	1.3764 _{↓58.1%}	15.95 _{↑125.4%}	68.25
Softmax (Oquab et al., 2024)	SigLIP-L	512 ²	304.15	310.60	1.3181	36.52	70.57
Hedgehog (Zhang et al., 2024)	SigLIP-L	512 ²	305.72	265.41 _{↓14.5%}	1.2221 _{↓7.3%}	37.44 _{↑2.5%}	39.53
LoLCATS (Zhang et al., 2025)	SigLIP-L	512 ²	305.72	265.41 _{↓14.5%}	1.2221 _{↓7.3%}	37.44 _{↑2.5%}	23.09
Linformer (Wang et al., 2020)	SigLIP-L	512 ²	305.72	262.19 _{↓15.6%}	1.2221 _{↓7.3%}	45.41 _{↑25.3%}	21.81
Performer (Choromanski et al., 2021)	SigLIP-L	512 ²	304.15	265.41 _{↓14.6%}	1.2164 _{↓7.7%}	36.48 _{↑0.1%}	39.93
Cosformer (Qin et al., 2022)	SigLIP-L	512 ²	304.15	265.41 _{↓14.6%}	1.2226 _{↓7.2%}	39.55 _{↑8.2%}	40.56
Nyströmformer (Xiong et al., 2021)	SigLIP-L	512 ²	304.15	265.20 _{↓14.6%}	1.2163 _{↓7.7%}	18.29 _{↓50.8%}	43.52
Monarch (Yaras et al., 2025)	SigLIP-L	512 ²	304.15	269.44 _{↓13.3%}	1.2304 _{↓6.7%}	18.31 _{↓48.9%}	43.94
ViT-AdaLA (Stage 2)	SigLIP-L	512 ²	304.15	262.19 _{↓15.6%}	1.2163 _{↓7.7%}	41.56 _{↑16.1%}	67.35
ViT-AdaLA (Ours)	SigLIP-L	512 ²	304.15	262.19 _{↓15.6%}	1.2163 _{↓7.7%}	41.56 _{↑16.1%}	68.20
Softmax (Oquab et al., 2024)	SigLIP-L	1024 ²	304.15	1241.0	3.2836	7.07	76.53
Hedgehog (Zhang et al., 2024)	SigLIP-L	1024 ²	305.72	442.24 _{↓64.4%}	1.3823 _{↓57.9%}	15.38 _{↑117.4%}	40.17
LoLCATS (Zhang et al., 2025)	SigLIP-L	1024 ²	305.72	442.24 _{↓64.4%}	1.3823 _{↓57.9%}	15.38 _{↑117.4%}	24.56
Linformer (Wang et al., 2020)	SigLIP-L	1024 ²	305.72	429.35 _{↓65.4%}	1.3999 _{↓57.4%}	17.83 _{↑152.0%}	6.92
Performer (Choromanski et al., 2021)	SigLIP-L	1024 ²	304.15	442.24 _{↓64.4%}	1.3765 _{↓58.1%}	15.23 _{↑115.3%}	40.53
Cosformer (Qin et al., 2022)	SigLIP-L	1024 ²	304.15	442.24 _{↓64.4%}	1.3945 _{↓57.5%}	15.29 _{↑116.1%}	39.90
Nyströmformer (Xiong et al., 2021)	SigLIP-L	1024 ²	304.15	442.24 _{↓64.4%}	1.3764 _{↓58.1%}	14.61 _{↑106.5%}	41.86
Monarch (Yaras et al., 2025)	SigLIP-L	1024 ²	304.15	500.24 _{↓59.7%}	1.5469 _{↓52.9%}	9.74 _{↑37.6%}	46.58
ViT-AdaLA (Stage 2)	SigLIP-L	1024 ²	304.15	429.35 _{↓65.4%}	1.3764 _{↓58.1%}	15.95 _{↑125.4%}	72.41
ViT-AdaLA (Ours)	SigLIP-L	1024 ²	304.15	429.35 _{↓65.4%}	1.3764 _{↓58.1%}	15.95 _{↑125.4%}	73.33

Table 12. mIoU fine-tuning comparison on ADE20K under ViT-IN1K and SigLIP with multiple linear attention baselines. We reproduce all baselines to ensure a fair comparison. The segmentation head is Mask2former for all the methods.

	Backbone	Res.	Params (M)	FLOPS (G)	Peak Mem. (GB)	Throughput (imgs/s)	mIoU (%)
Softmax (Oquab et al., 2024)	IN1K ViT-L	512 ²	304.20	310.60	1.3181	36.52	50.83
Hedgehog (Zhang et al., 2024)	IN1K ViT-L	512 ²	305.77	265.41 _{↓14.5%}	1.2221 _{↓7.3%}	37.44 _{↑2.5%}	25.15
LoLCATS (Zhang et al., 2025)	IN1K ViT-L	512 ²	305.77	265.41 _{↓14.5%}	1.2221 _{↓7.3%}	37.44 _{↑2.5%}	20.17
Linformer (Wang et al., 2020)	IN1K ViT-L	512 ²	305.77	262.19 _{↓15.6%}	1.2221 _{↓7.3%}	45.41 _{↑25.3%}	11.49
Performer (Choromanski et al., 2021)	IN1K ViT-L	512 ²	304.20	265.41 _{↓14.6%}	1.2164 _{↓7.7%}	36.48 _{↑0.1%}	31.01
Cosformer (Qin et al., 2022)	IN1K ViT-L	512 ²	304.20	265.41 _{↓14.6%}	1.2226 _{↓7.2%}	39.55 _{↑8.2%}	29.65
Nyströmformer (Xiong et al., 2021)	IN1K ViT-L	512 ²	304.20	265.20 _{↓14.6%}	1.2163 _{↓7.7%}	18.29 _{↓50.8%}	41.67
Monarch (Yaras et al., 2025)	IN1K ViT-L	512 ²	304.20	269.44 _{↓13.3%}	1.2304 _{↓6.7%}	18.31 _{↓48.9%}	45.05
ViT-AdaLA (Stage 2)	IN1K ViT-L	512 ²	304.20	262.19 _{↓15.6%}	1.2163 _{↓7.7%}	41.56 _{↑16.1%}	46.92
ViT-AdaLA (Ours)	IN1K ViT-L	512 ²	304.20	262.19 _{↓15.6%}	1.2163 _{↓7.7%}	41.56 _{↑16.1%}	49.75
Softmax (Oquab et al., 2024)	SigLIP-L	512 ²	304.20	310.60	1.3181	36.52	54.4
Hedgehog (Zhang et al., 2024)	SigLIP-L	512 ²	305.77	265.41 _{↓14.5%}	1.2221 _{↓7.3%}	37.44 _{↑2.5%}	22.13
LoLCATS (Zhang et al., 2025)	SigLIP-L	512 ²	305.77	265.41 _{↓14.5%}	1.2221 _{↓7.3%}	37.44 _{↑2.5%}	20.11
Linformer (Wang et al., 2020)	SigLIP-L	512 ²	305.77	262.19 _{↓15.6%}	1.2221 _{↓7.3%}	45.41 _{↑25.3%}	12.37
Performer (Choromanski et al., 2021)	SigLIP-L	512 ²	304.20	265.41 _{↓14.6%}	1.2164 _{↓7.7%}	36.48 _{↑0.1%}	23.97
Cosformer (Qin et al., 2022)	SigLIP-L	512 ²	304.20	265.41 _{↓14.6%}	1.2226 _{↓7.2%}	39.55 _{↑8.2%}	23.08
Nyströmformer (Xiong et al., 2021)	SigLIP-L	512 ²	304.20	265.20 _{↓14.6%}	1.2163 _{↓7.7%}	18.29 _{↓50.8%}	32.54
Monarch (Yaras et al., 2025)	SigLIP-L	512 ²	304.20	269.44 _{↓13.3%}	1.2304 _{↓6.7%}	18.31 _{↓48.9%}	38.87
ViT-AdaLA (Stage 2)	SigLIP-L	512 ²	304.20	262.19 _{↓15.6%}	1.2163 _{↓7.7%}	41.56 _{↑16.1%}	51.39
ViT-AdaLA (Ours)	SigLIP-L	512 ²	304.20	262.19 _{↓15.6%}	1.2163 _{↓7.7%}	41.56 _{↑16.1%}	53.55